Supporting Information

CoO_x modified $SnNb_2O_6$ Photoelectrode for Highly Efficient Oxygen Evolution from Water

Ryo Niishiro,[a,b] Yuichi Takano,[b] Qingxin Jia,[c] Masaharu Yamaguchi,[c] Akihide Iwase,[d] Yongbo Kuang,[c] Tsutomu Minegishi,[c] Taro Yamada,[c] Kazunari Domen[c] and Akihiko Kudo[d,*]

[a]Mitsui Chemicals, Inc., 580-32 Nagaura, Sodegaura, Chiba 299-0265, Japan

[b]Japan Technological Research Association of Artificial Photosynthetic Chemical Process (ARPChem), 2-11-9 Iwamotocho, Chiyoda-ku, Tokyo 101-0032, Japan

[c]Department of Chemical System Engineering, The University of Tokyo, 7-3-1 Hongo, Bunkyo-ku, Tokyo 113-8656, Japan

[d]Department of Applied Chemistry, Faculty of Science, Tokyo University of Science, 1-3 Kagurazaka, Shinjuku-ku, Tokyo 162-8601, Japan

Experimental

Characterization

Crystal phases of the obtained powders were confirmed using X-ray diffraction (Rigaku; SmartLab, Cu $K\alpha$). The X-ray diffraction (XRD) patterns were collected from 5° to 70° (2θ) using a step size 0.02°. The source power and current of Cu $K\alpha$ radiation were 40 kV and 30 mA, respectively. Diffuse reflection spectra (DRS) were obtained using a UV-VIS-NIR spectrometer (JASCO; V-670) and were converted from reflectance to absorbance by the Kubelka-Munk method. Photocatalyst powders and phoelectrodes were observed using a scanning electron microscope (Hitachi High-Technologies; SU8020). Focused ion beam (SEIKO Instruments; SMI2050) was used to cut photoelectrodes for the cross-section observation.

Calculations

$E_{Ag/AgCl}$ was converted to E_{RHE} according the following equation.

$$E_{RHE}[\mathrm{V}] = (E_{Ag/AgCl} + 0.199 + 0.059 \times \mathrm{pH})[\mathrm{V}] \qquad (\mathrm{eq.\,S1})$$

IPCE was determined by the following equation.

$$\mathrm{IPCE}[\%] = \frac{J[\mathrm{mA/cm^2}] \times 1240[\mathrm{V \times nm}]}{P_{mono}[\mathrm{mW/cm^2}] \times \lambda[\mathrm{nm}]} \times 100 \qquad (\mathrm{eq.\,S2})$$

Here, P_{mono}, and λ represent intensity and wavelength of incident monochromatic light, respectively.

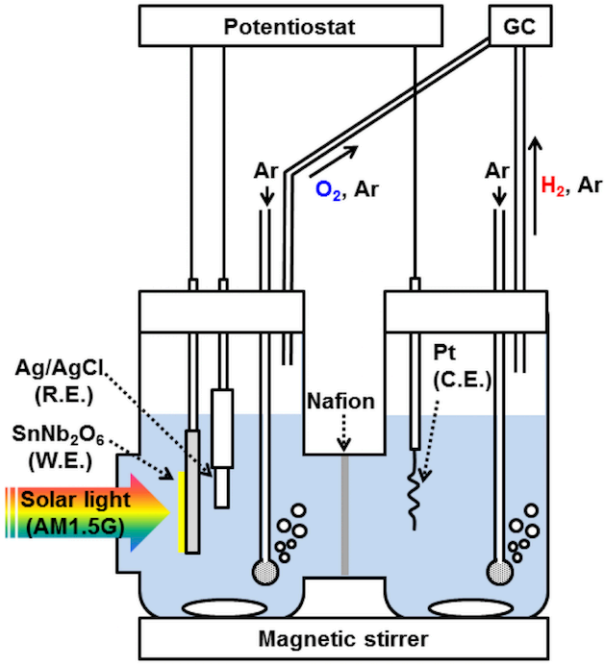

Fig. S1 H-type cell for photoelectrochemical measurement equipped with an on-line gas chromatography.

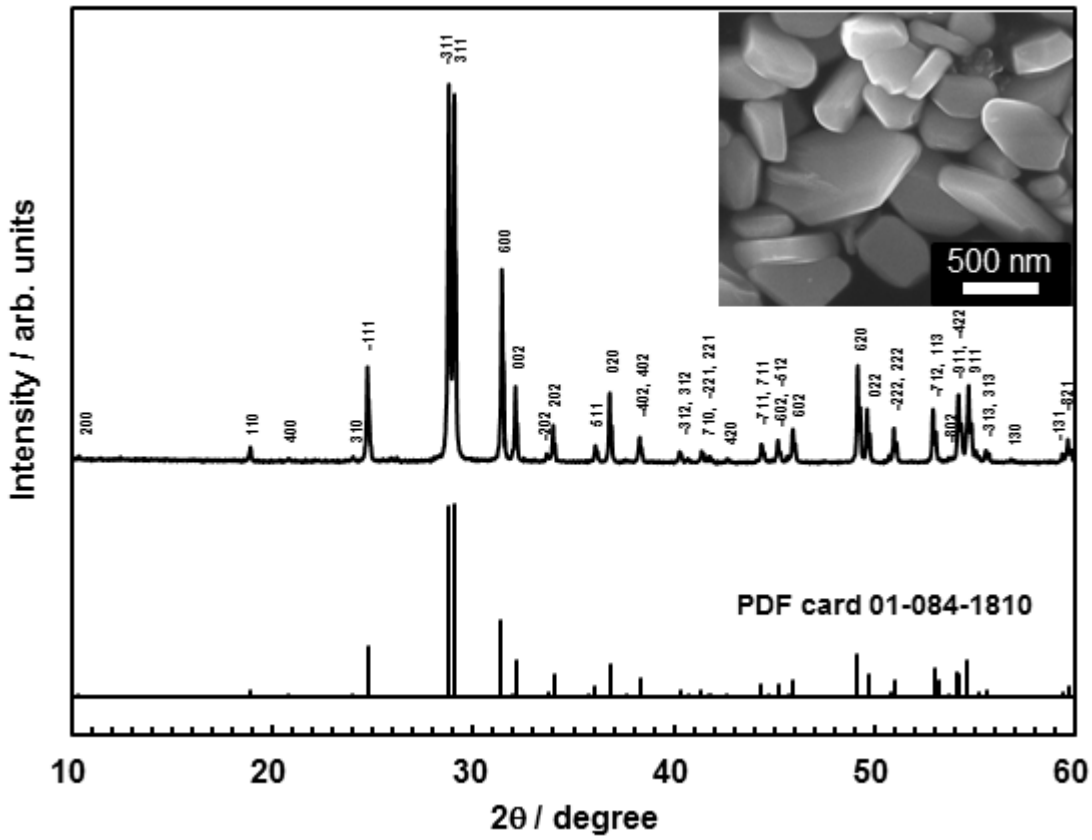

Fig. S2 An X-ray diffraction pattern of $SnNb_2O_6$ photocatalyst powder. The inset shows an SEM image of $SnNb_2O_6$ photocatalyst powder.

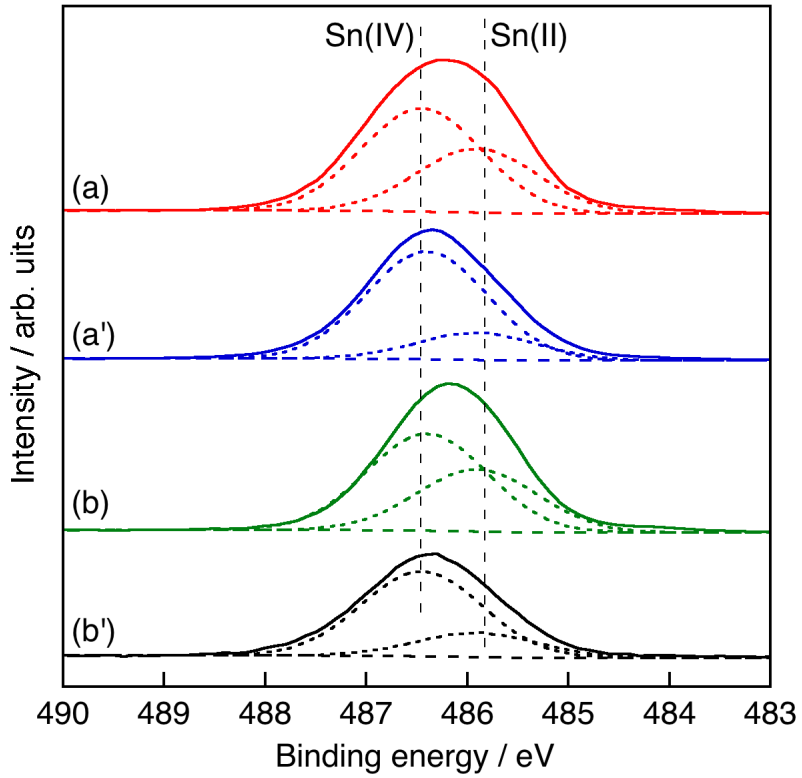

Fig. S3 XPS spectra of $Sn3d_{5/2}$ of (a, a') non-loaded and (b, b') CoO_x-loaded $SnNb_2O_6$ photoelectrodes (a, b) before and (a', b') after photoelectrochemical measurements.

Table S1 XPS areas of Sn^{2+} and Sn^{4+} ions and calculated proportions of Sn^{2+} ions at the surface of non-loaded and CoO_x-loaded $SnNb_2O_6$ photoelectrodes.

sample	measurement	XPS area		proportion of Sn^{2+}
		Sn^{2+}	Sn^{4+}	
non-loaded $SnNb_2O_6$	before	53000	33000	0.38
non-loaded $SnNb_2O_6$	after	55500	14000	0.20
CoO_x-loaded $SnNb_2O_6$	before	50000	32000	0.39
CoO_x-loaded $SnNb_2O_6$	after	17500	5000	0.22

[Proportion of Sn^{2+}]=[XPS area of Sn^{2+}]/([XPS area of Sn^{2+}] + [XPS area of Sn^{4+}])

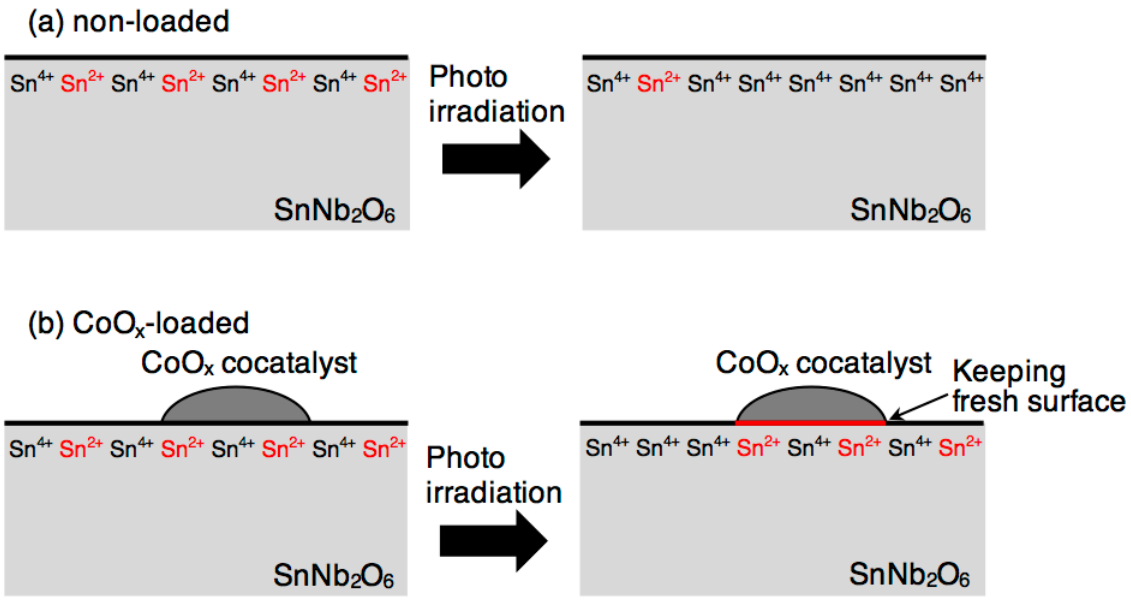

Fig. S4 Schematic of chemical states of Sn species at the surface of non-loaded and CoO_x-loaded $SnNb_2O_6$ photoelectrodes before and after photoelectrochemical measurements.

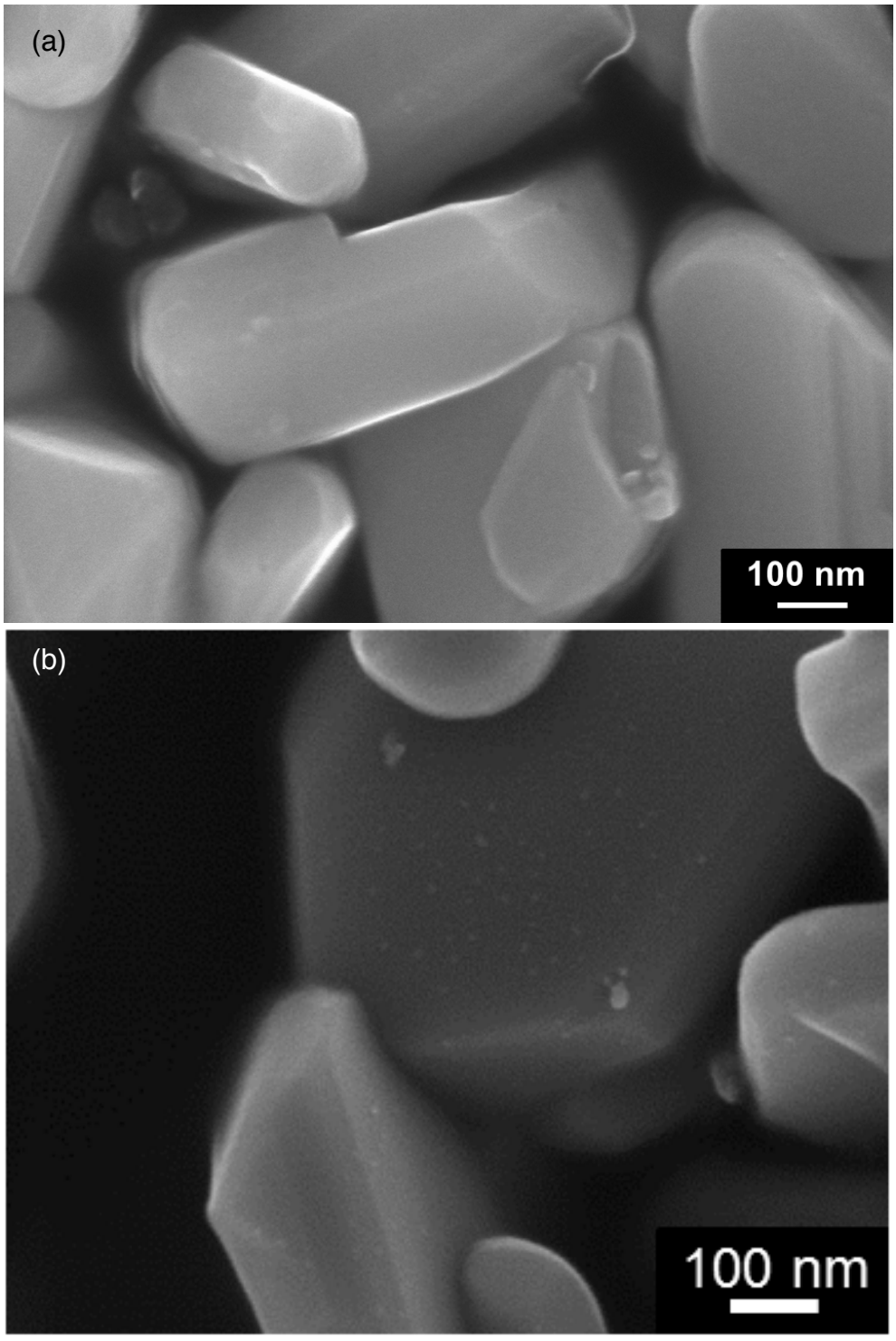
(a)
100 nm
(b)
100 nm

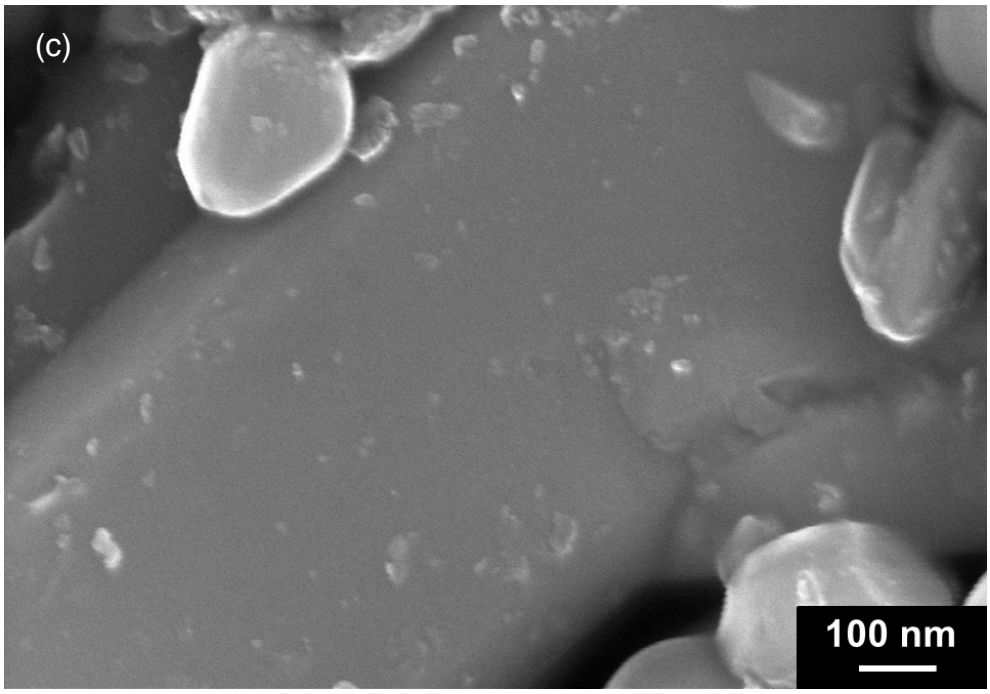

Fig. S5 SEM images of (a) non-loaded, (b) CoO_x(0.5 wt%)-loaded, and (c) CoO_x(1.0 wt%)-loaded $SnNb_2O_6$ photocatalysts. The calcination temperature in air for loading of CoO_x cocatalyst was 473 K.

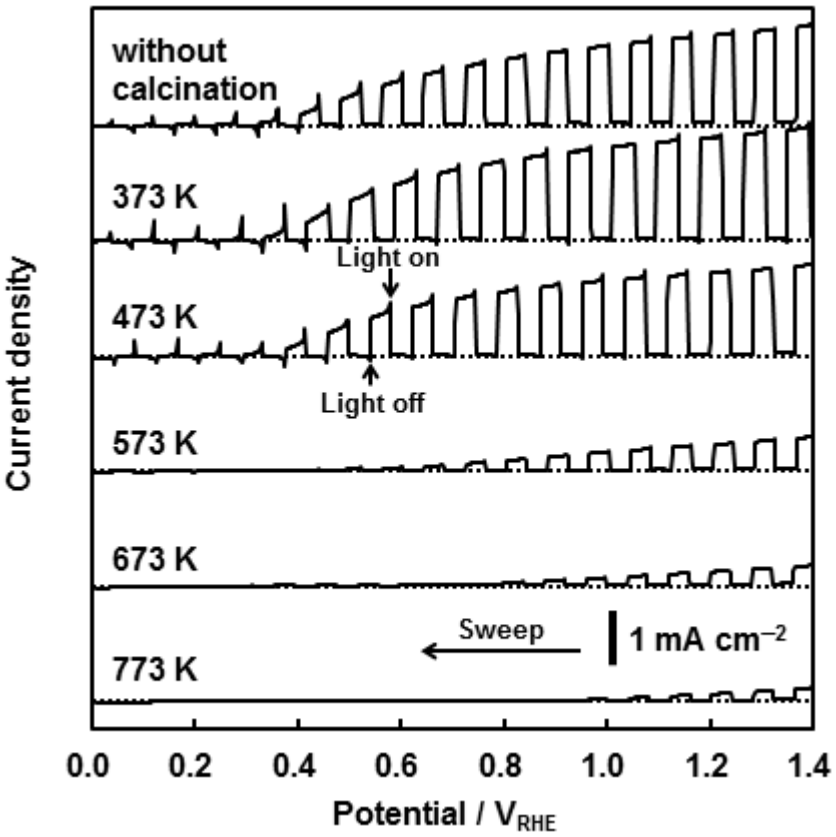

Fig. S6 Effect of calcination temperature in air for loading of a CoO_x cocatalyst on the photoelectrochemical performance of a CoO_x(0.5wt%)/$SnNb_2O_6$ photoanode. Electrolyte, 0.125 mol L^{-1} $K_2B_4O_7$ aqueous solution (pH 9.4); light source, solar simulator (AM 1.5G, 100 mW cm^{-2}).

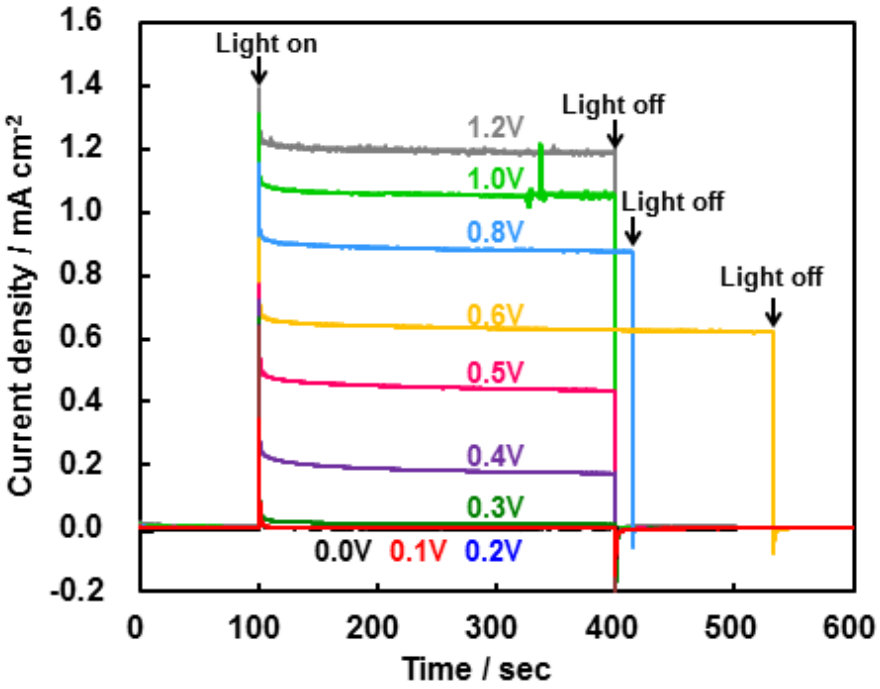

Fig. S7 Time courses of photocurrent of a CoO_x(0.5wt%)/$SnNb_2O_6$ photoelectrode at 0.0–1.2 V_{RHE}. Electrolyte, 0.125 mol L^{-1} $K_2B_4O_7$ aqueous solution (pH 9.4); light source, solar simulator (AM 1.5G, 100 mW cm^{-2}).